Integration of Copernicus Data and Services to Assess Local Aridity Conditions in the Apulian Context: The Case of Marina di Ginosa

Carlo Barletta, Alessandra Capolupo(✉), and Eufemia Tarantino

Department of Civil, Environmental, Land, Building Engineering and Chemistry (DICATECh), Politecnico Di Bari, Via Orabona 4, 70125 Bari, Italy
{carlo.barletta,alessandra.capolupo,eufemia.tarantino}@poliba.it

Abstract. Water is a fundamental element for life on the Earth. Its availability, at a local scale, depends on the climate as well as on how it is managed and distributed for human use. Nowadays, water scarcity is a major concern in many parts of the world, also in relation to the possible effects of climate change and urbanization. The aim of this study is to integrate various Copernicus and other free and open data in order to calculate the main components of the water balance as defined by ISPRA's BIGBANG procedure. The territory of a basin including the locality of Marina di Ginosa, in southern Italy, was chosen as study site. All the analyses were carried out in the Google Earth Engine cloud environment, where a proper JavaScript code was developed. The estimation made it possible to retrieve monthly maps of the hydrological variables from October 2015 to September 2018 at a geometric resolution of 10 m, and to assess local drought conditions by applying the FAO-UNEP aridity index. Even if this approach is affected by uncertainties owing to the schematic representation of the natural processes, it is a valuable tool for analyzing the spatial and temporal fluctuations of the water resource availability, especially in critical areas of southern Italy.

Keywords: GEE · Climate change · BIGBANG · desertification · drought

1 Introduction

In the next future, climate change is expected to affect the water availability for human consumption and ecosystems, leading to possible changes in the hydrological cycle and, therefore, resulting in drier conditions than in the past, especially in the semi-arid regions of southern Europe. Soil-water dynamics depend on various complex hydro-meteorological and biophysical processes, that control the hydrological balance. Indeed, not all the water that flows into a catchment area infiltrates the soil; following a conceptual scheme, there is also a part of the precipitation that runs off the soil surface and another one that returns to the atmosphere through the process of evapotranspiration. Additionally, the soil-water interaction is affected by multiple factors (climatic conditions, soil physical properties, topography, land cover, soil management practices etc.).

© The Author(s), under exclusive license to Springer Nature Switzerland AG 2023
O. Gervasi et al. (Eds.): ICCSA 2023 Workshops, LNCS 14107, pp. 201–216, 2023.
https://doi.org/10.1007/978-3-031-37114-1_14

Climate change may endanger the amount of water in the soil for social and economic activities because of natural and anthropogenic causes, as well as variations in land use/land cover (LU/LC) [1–12].

A quantitative examination of the water balance components using models is a good technique to evaluate the impacts of climate change and urbanization on aridity conditions of soils and, thus, on water resource availability. For this purpose, the Italian National Institute for Environmental Protection and Research (ISPRA) developed the "Nationwide GIS-based regular gridded hydrological water budget" procedure, called BIGBANG, which allows the monthly evaluation of the water balance components for the Italian territory through a spatially distributed approach, with a resolution of 1 km. This model employs basic and well-established approaches from the literature, requiring only a few parameters [1, 7–9, 11, 13–15]. However, in order to enhance the analysis at the local scale, it would be essential to develop a tool that allows for a better understanding of the spatial and temporal variability of these processes at a higher geometric resolution. This would aid in water management and planning for resource protection purposes.

Today, a significant source of data and information for environmental analysis and monitoring is provided by the Copernicus initiative of the European Union (EU). The Copernicus collection consists of multispectral and radar imagery acquired by the Sentinel satellites (namely the "space component"), in-situ observations from contributing missions which are provided by international and national agencies or by private entities (the so called "in-situ component"), and value-added information from the "services component", which is made up of six thematic services (marine, land, atmosphere, emergency, climate change and security) [16, 17]. The Copernicus Climate Change Service (C3S) provides data and information in a free and open format to support the analysis of climate change impacts and the EU's adaptation and mitigation policies. The C3S is based on existing research infrastructures and knowledge available worldwide, and allows its users to freely access to a variety of climate datasets in the Climate Data Store (https://cds.climate.copernicus.eu) [18, 19]. On the other hand, the Copernicus Land Monitoring Service (CLMS) provides data and information on LU/LC and biophysical parameters at the European scale with a resolution of 10 m (https://land.copernicus.eu/pan-european/high-resolution-layers), as well as other data such as the 25 m resolution pan-European digital surface model (the "EU-DEM", available at https://land.copernicus.eu/imagery-in-situ/eu-dem/eu-dem-v1-0-and-derived-products).

The aim of this work is to integrate different free and open data provided by Copernicus program with other open informative layers, provided by national or international institutions, in order to retrieve the main water balance components, as defined by the ISPRA BIGBANG procedure, on a local scale and with a geometric resolution of 10 m. This approach, which allows for the spatial and temporal analysis of the variability of the water balance components, could be a useful tool for the detailed assessment of local aridity conditions, particularly in areas of southern Italy at risk of desertification and drought, as well as to support a sustainable water resource management.

The basin's region, including the area of Marina di Ginosa in southern Italy, was chosen as the research site since it was feasible to download Copernicus data of monthly

temperature and precipitation readings from 2015 to 2018. Unlike the ISPRA's BIGBANG model, which was developed in ArcGIS software, this study was carried out by creating and implementing a JavaScript code in the Google Earth Engine (GEE) cloud platform, a free-to-use environment developed by Google for analyzing and handling a large volume of geospatial and Earth Observation (EO) data using Google's high performance computing capabilities [20–24]. The proposed methodology, which takes advantage of the cloud technology, can speed-up the operations and computations required to obtain the results.

2 Materials and Methods

2.1 Study Area and Data

The basin including the location of Marina di Ginosa, mainly belonging to the Apulia Region and, in a very small part, to the Basilicata Region, was selected as pilot site because monthly observations of air temperature and precipitation were available from a Copernicus dataset for the period 2015–2018. The study area, located between the Bradano and Lato river basins, is part of the "Ionian Arc of Taranto", in the southern sector of a foreland basin called "Bradanic Trough" (Fig. 1).

From a geomorphological point of view, this territory is characterized by a succession of marine terraces consisting of discontinuous strips of terraced marine deposits, marly grey-blue clays, calcarenites, alluvial deposits and coastal dunes resting on calcareous rocks [25, 26].

The investigated territory covers an area of 116.2 km^2, with a maximum elevation of 92.4 m above sea level (a.s.l.) and is crossed by the Galaso stream.

The climate is typically Mediterranean, characterized by fairly hot (maximum temperatures >30–35 °C) and dry summers, and mild winters. Precipitation is mostly concentrated in the autumn-winter period; its average annual amount, in the Taranto area, is often less than 500 mm/year. In general, only the autumn-winter precipitation contributes to the aquifer recharge since the scarce summer rainfall is significantly lost for evapotranspiration. In addition, in this area of the Apulia Region, rainfall characterized by high intensity prevail, minimally contributing to the groundwater recharge and causing sudden and occasional surface runoff [27].

The LU/LC of the study area was preliminarily analyzed using the Copernicus "CORINE land cover 2018" dataset (where CORINE stands for COoRdination of INformation for the Environment), available on the CLMS website with a geometric resolution of 100 m [28]. The distribution of the LU/LC categories is detailed in Table 1: the 84.6% of the territory is dedicated to agricultural use while only 7.1% of the total area is destinated for the artificial surfaces.

To calculate the main components of the hydrological balance, monthly observations of four variables (maximum, minimum and mean temperature, and precipitation), measured by the hydro-meteorological station of Marina di Ginosa, and available in the Climatic Research Unit (CRU) v.4.06 dataset [29] (https://cds.climate.copernicus.eu/cdsapp#!/dataset/insitu-gridded-observations-global-and-regional?tab=overview) were

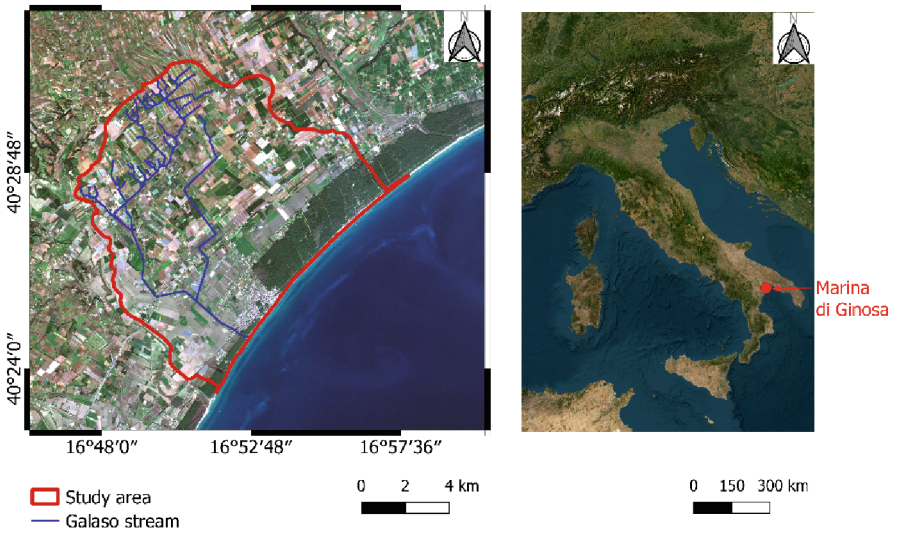


Fig. 1. Study area.

Table 1. Distribution of LU/LC classes according to CORINE land cover 2018 dataset.

	CORINE land cover class	Area [km^2]	Percentage [%]
Artificial surfaces	Continuous urban fabric	1.2	1.0
	Discontinuous urban fabric	6.2	5.3
	Dump sites	0.6	0.5
	Sport and leisure facilities	0.3	0.3
Agricultural areas	Non-irrigated arable land	34.5	29.7
	Vineyards	30.8	26.5
	Fruit trees and berry plantations	8.9	7.7
	Pastures	0.4	0.3
	Complex cultivation patterns	23.7	20.4
Forest and semi natural areas	Coniferous forest	5.6	4.8
	Sclerophyllous vegetation	3.6	3.1
	Beaches, dunes, sands	0.4	0.3

selected. Because there were no missing data in the dataset for these years, the evaluation was limited to the years 2015–2018. Moreover, the monthly temperature and precipitation values were considered constant over the entire study area.

The soil sealing maps, produced by ISPRA from the CLMS Imperviousness layers (https://land.copernicus.eu/pan-european/high-resolution-layers/imperviousness) at 10 m resolution, are essential for the implementation of the BIGBANG model [13,

30]. Because this project spanned the years 2015 to 2018, four layers, corresponding to soil sealing maps for 2015, 2016, 2017, and 2018, were acquired from the ISPRA web page (https://groupware.sinanet.isprambiente.it/uso-copertura-e-consumo-di-suolo/library/consumo-di-suolo). These classified maps were then aggregated in the GEE platform into two main macro-classes: "Impervious surface" and "Non impervious surface". Figure 2 illustrates one of the four soil sealing maps obtained in GEE after aggregating the various LU/LC classes.

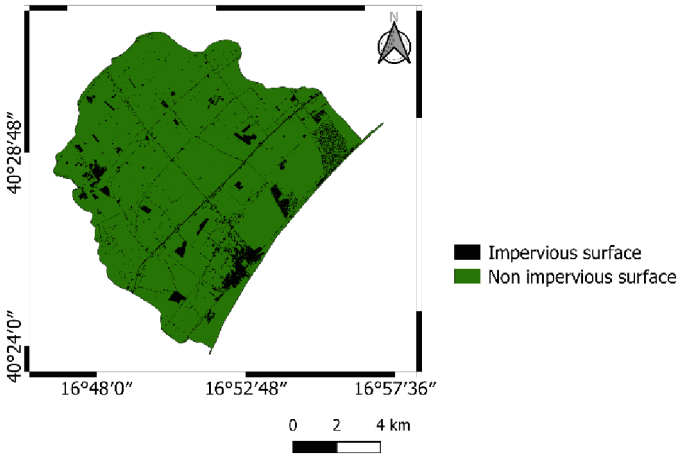


Fig. 2. The soil sealing map 2015, obtained in GEE for the study area, after aggregating the various LU/LC classes into two main categories.

Other necessary data for this work are the map of the Available Water Capacity (AWC) of the soil and the map of the Potential Infiltration Coefficient (CIP) [13]. The former, produced by the European Soil Data Center (ESDAC) [31–34] is an open data with 500 m resolution (https://esdac.jrc.ec.europa.eu/content/topsoil-physical-properties-europe-based-lucas-topsoil-data). The latter, was derived from the Mouton hydrogeological complexes map produced by ISPRA (http://www.sinanet.Isprambiente.it/it/sia-ispra/download-mais/complessi-idrogeologici/view) assigning a CIP value to each complex as reported by Celico (1998) [13, 35].

2.2 GEE and Operative Workflow

GEE is a free cloud platform that exploits Google's computational infrastructure to allow to analyze large geospatial data sets for environmental monitoring and analysis while minimizing operational and computational time. To achieve the objectives of this study, a proper code was created and implemented in the GEE Code Editor, the Integrated Development Environment (IDE) designed for the development of algorithms using the JavaScript programming language [22, 36, 37].

Figure 3 describes the operative workflow used in this investigation.

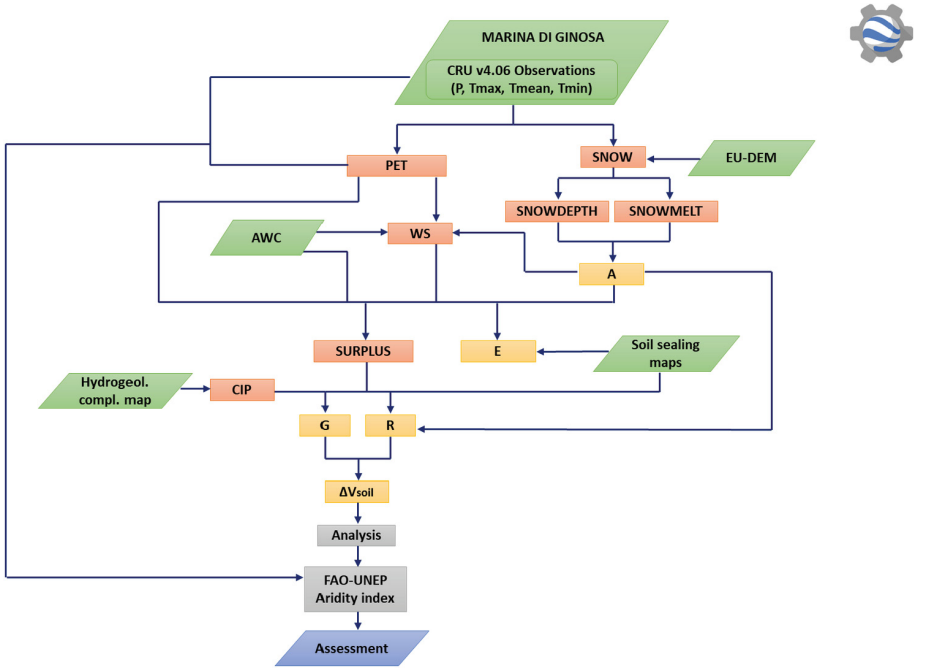


Fig. 3. Operative workflow. CRU: Climatic Research Unit; P: Precipitation; T_{max}: Maximum Temperature; T_{mean}: Mean Temperature; T_{min}: Minimum Temperature; PET: Potential Evapotranspiration; EU-DEM: European Union-Digital Elevation Model; AWC: Available Water Capacity; WS: Soil Water Content; A: Liquid Inflow; E: Actual Evapotranspiration; CIP: Potential Infiltration Coefficient; G: Groundwater Recharge; R: Surface Runoff; ΔV_{soil}: Variation in Soil Water Content; FAO: Food and Agriculture Organization; UNEP: United Nations Environmental Programme.

After selecting the monthly values of total precipitation (P), and the monthly means of daily maximum, mean and minimum air temperature (T_{max}, T_{mean} and T_{min}) from the CRU v4.06 dataset [29], related to the "Marina di Ginosa" meteorological station, four thematic maps of P, T_{max}, T_{mean} and T_{min} were obtained in the GEE environment for each month from October 2015 to September 2018. This was done to perform the analysis considering three hydrological years (2015–2016, from October 2015 to September 2016; 2016–2017, from October 2016 to September 2017; and 2017–2018, from October 2017 to September 2018). Furthermore, for each month i, it was decided to keep the monthly values of P_i, $T_{max,i}$, $T_{mean,i}$ and $T_{min,i}$ constant over the whole study area, due to the similar morphological and climatic characteristics of the whole territory, which is also relatively small.

Then, from P, T_{max}, T_{mean} and T_{min}, the maps of potential evapotranspiration (PET) and liquid inflow A were calculated for each month. The EU-DEM was used to obtain the possible monthly snow precipitation from which it is possible to derive the values of monthly snow accumulation and snowmelt, as reported in [13]. The PET and A maps were then used together with the AWC data to retrieve the soil water content (WS), the

actual evapotranspiration E and the surplus, for each month. The 10 m resolution soil sealing maps were used to perform the calculation separately for "impervious" and "non impervious" classes. Moreover, the maps of groundwater recharge G and surface runoff R were calculated for each month from the CIP data, together with the surplus, A and the soil sealing maps. Then, it was possible to retrieve the variation of the soil water content for each of the investigated month. Lastly the assessment of the soil aridity conditions, for each hydrological year (2015–2016, 2016–2017, and 2017–2018) was performed by calculating the FAO-UNEP aridity index [13].

2.3 Water Balance Components Computation

According to the BIGBANG procedure, considering a generic month i, the water balance for the root zone (the layer of soil that is affected by the root system of the vegetation), is expressed as follows [13]:

$$A - E = R + G + \Delta V_{soil} \tag{1}$$

where

- A is the volume of the liquid inflow that reaches the soil, consisting of the rainfall plus the snowmelt;
- E is the volume of the actual evapotranspiration;
- R is the volume of the surface runoff;
- G is the volume of the groundwater recharge;
- ΔV_{soil} is the variation of the volume of stored water in the soil;

Once obtained, for each month i, the thematic maps of precipitation and temperature (considered constant over the entire study area) from October 2015 to September 2018, the following variables were retrieved:

- Liquid inflow A;
- Potential evapotranspiration PET;
- Soil water content WS;
- Actual evapotranspiration E;
- Groundwater recharge G;
- Surface runoff R;
- Soil water content variation ΔV_{soil}.

Liquid Inflow Because the average temperature for each month studied is always higher than the threshold for snow formation, there is no melting, and the liquid inflow A_i always corresponds with the total monthly precipitation (P_i).

Potential Evapotranspiration. This variable, expressed in mm/month, was calculated, for each month i, with the equation of Hargreaves and Samani [13]:

$$PET_i = M_i * 0.0135 * [T_{mean,i} + 17.8] * [0.17 * \sqrt{T_{\max,i} - T_{\min,i}} * R_{a,i}] \tag{2}$$

where

- M_i is the number of days of the month i;

- $T_{mean,i}$, $T_{max,i}$, $T_{min,i}$ are the monthly mean of daily mean, maximum and minimum temperature [°C], for the month i;

- $R_{a,i}$ is the monthly mean of the daily extraterrestrial radiation [mm/day of evaporated water equivalent], for the month i, calculated as in [13].

Soil Water Content. The water content in the soil depth of 1 m was computed using the scheme reported in [13]:

$$WS_i = f(A_i, PET_i, AWC, WS_{i-1}) \tag{3}$$

where

- AWC is the available water capacity [mm of water/m of soil depth];
- WS_{i-1} [mm/m] is the soil water content in the month i–1.

Since, in this model, an initial condition is required, it was assumed that in January 2015 the soil water content was equal to AWC over the entire case study territory.

Actual Evapotranspiration. The soil sealing maps at 10 m resolution were used to compute the actual evapotranspiration, for each month i, differently for "Impervious surface" and "non impervious surface" LU/LC classes.

For "impervious surface" class, according to [13]:

$$E_i = 0 \tag{4}$$

as it was assumed that these areas are without vegetation (no transpiration) and that all the liquid inflow turns into surface runoff.

For "non impervious surface" LU/LC class, instead, the expressions reported in [13] were adopted:

$$E_i = f(A_i, PET_i, AWC, WS_{i-1}) \tag{5}$$

Groundwater Recharge. In Order to Determine the Groundwater Recharge G, for Each month i, the Surplus (from Which G is Generated) Was First Calculated Using the Following Expression [13]:

$$Surplus_i = \max\{[(A_i - PET_i) - (AWC - WS_{i-1})], 0\} \tag{6}$$

Then, the G was computed in this way: for "Impervious surface" LU/LC class

$$G_i = 0 \tag{7}$$

while, for "Non impervious surface" class, the following equation was considered

$$G_i = \frac{CIP}{100} * Surplus_i \tag{8}$$

where CIP is the potential infiltration coefficient.

Surface Runoff. The Runoff, for the month i, Was Calculated [13]:

For "Impervious surface class"

$$R_i = A_i \tag{9}$$

and, for "Non impervious surface" class, as complementary

$$R_i = \left(1 - \frac{CIP}{100}\right) * Surplus_i \tag{10}$$

Variation in Soil Water Content. The Soil Water Content Variation, for Each month i, Was Retrieved by Using the Following Expression [13]:

$$\Delta V_{soil,i} = A_i - E_i - R_i - G_i \tag{11}$$

2.4 Soil Aridity Assessment

The assessment of the soil aridity condition was performed by calculating, for each hydrological year (2015–2016, 2016–2017 and 2017–2018) and for the entire period of analysis (from October 2015 to September 2018), the aridity index (AI) proposed by Food and Agriculture Organization (FAO) and United Nations Environmental Programme (UNEP) [13, 38], expressed by:

$$AI_{FAO-UNEP} = \frac{\overline{P}}{\overline{PET}} \tag{12}$$

where

- $\overline{P}$ is the mean annual precipitation [mm];
- $\overline{PET}$ is the mean annual potential evapotranspiration [mm].

The AI is a numerical indicator of aridity widely adopted for measuring the dryness of the climate at a given location. According to this index, the climate can be classified into the following types [13, 38–40]:

Table 2. Climate classification and dryland subtypes based on the FAO-UNEP aridity index.

Climate type	Subtype	Aridity index
Dry	Hyper-arid	AI < 0.05
	Arid	0.05 ≤ AI < 0.2
	Semi-arid	0.2 ≤ AI < 0.5
	Dry-subhumid	0.5 ≤ AI < 0.65
Non dry	Humid	AI ≥ 0.65

3 Results and Discussion

This research aimed at integrating various open Copernicus data in order to estimate, on a monthly scale, the components of the water balance, as defined by ISPRA's BIGBANG model [13], over the territory of Marina di Ginosa, in southern Italy, in order to assess the local aridity conditions.

As explained above, monthly maps of each variable were obtained by developing and implementing a JavaScript code in the GEE cloud environment, considering the period between October 2015 and September 2018. Therefore, it was possible to perform the analysis for three hydrological years: 2015–2016, 2016–2017 and 2017–2018.

Table 3 and Fig. 4 summarize the results of this study. Table 3 reports the annual values of A, E, R, G and ΔV_{soil} at the level of the whole study area. Figure 4A shows the annual water balance while, in Fig. 4B is represented the trend of the monthly mean values of A, E, R and G over the case study area. According to Table 3 and Fig. 4A, the wettest year was the 2015–2016 (A = 534 mm), while the driest year was the 2017–2018 (only 392 mm). Furthermore, based on the model, a considerable portion of the precipitation was owing to evapotranspiration in all three hydrological years and groundwater recharge was nil in 2015–2016 and 2017–2018. On the other hand, the runoff is approximately 10% of the inflow in all cases, while a value of ΔV_{soil} of + 0.1 mm was found for each hydrological year from Eq. 11. As a result, for all three years, the input (A) was approximately equal to outputs (E, R and G).

However, if we calculate the difference between A and E (i.e. the "internal flow" [13, 41], which is a measure of the availability of the water resource generated, under natural conditions, exclusively by precipitation into a territory) it is possible to notice that the natural availability of the water resource for the area in question is very low, excluding external contributions (Table 4). The lowest availability of the resource was estimated in 2017–2018 (only 32.3 mm) and corresponds to the minimum of the annual inflow (see also Fig. 4).

Figure 4B shows the large monthly variability of precipitation, although groundwater recharge is different from zero only in January 2017, coinciding to the greatest precipitation reported at the Marina di Ginosa meteorological station. As an example, due to the impossibility of showing all the maps of the water balance components retrieved in the GEE platform, the Fig. 5 reports the annual average maps of E, R and G for the hydrological year 2016–2017. All the maps have been obtained with a geometric resolution of 10 m and allow for a local investigation of each component's variability within the case study region. The predicted values are dependent on the AWC parameter, which has a 500 m resolution, thus the maps appear to be at a lower resolution.

Table 3. Annual water balance, related to the whole study area, for the hydrological years 2015–2016, 2016–2017 and 2017–2018.

Year	A [mm]	E [mm]	R [mm]	G [mm]	ΔVsoil [mm]
2015–2016	534.0	490.1	43.8	0.0	+ 0.1
2016–2017	421.0	365.0	38.9	17.1	+ 0.1
2017–2018	392.0	359.7	32.2	0.0	+ 0.1

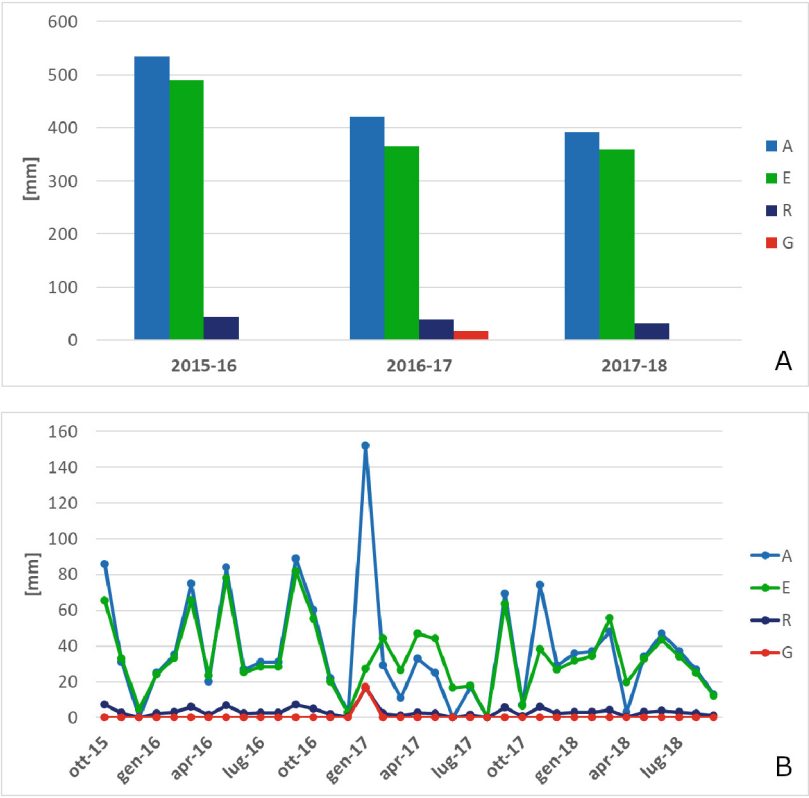


Fig. 4. Annual water balance, related to the whole study area, for the hydrological years 2015–2016, 2016–2017 and 2017–2018 (A), and monthly water balance for the whole study area (B).

Table 4. Internal flow, calculated by the difference between A and E, and annual mean temperature, related to the whole study area for the hydrological years 2015–2016, 2016–2017 and 2017–2018.

Year	Internal flow A [mm]	Annual mean temperature [°C]
2015–2016	43.9	18.0
2016–2017	56.0	18.0
2017–2018	32.3	17.9

It should be emphasized that the estimations are derived from a schematic representation of natural occurrences and so may therefore be susceptible to uncertainties. Further uncertainties could result from the extension of the monthly precipitation and temperature values, measured at the Marina di Ginosa station, to the entire study area. Furthermore, this assessment has not taken into account any anthropic contribution and any surface or underground contribution from external areas.

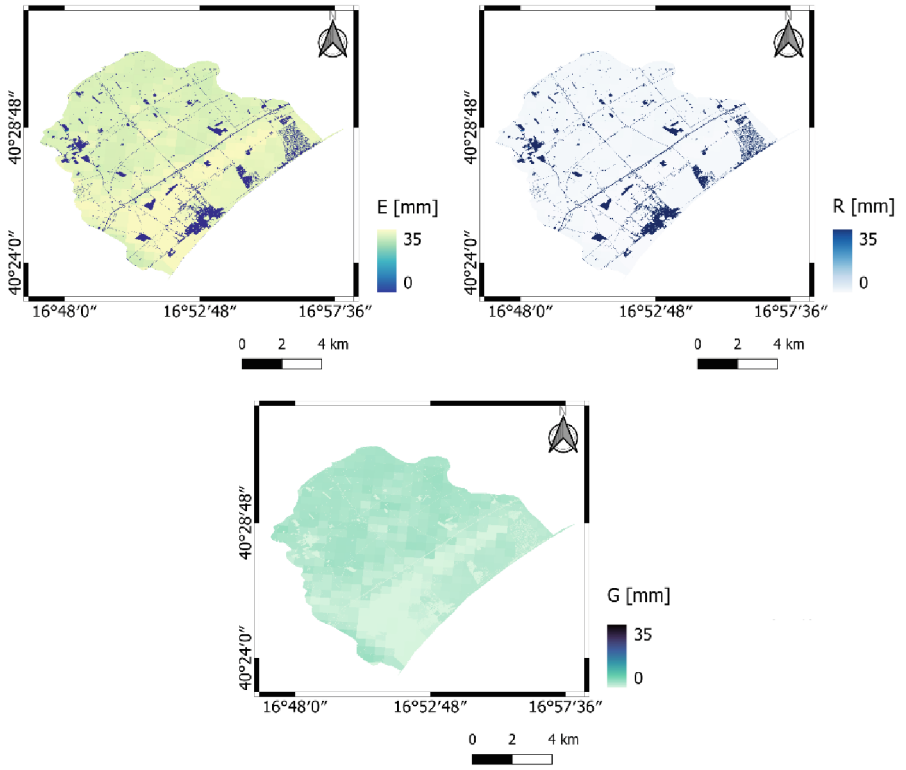


Fig. 5. Annual average maps of E, R and G for the hydrological year 2016–2017.

Table 5 reports the results of the application of the FAO-UNEP aridity index [13, 40]. In accordance with the thresholds reported in Table 2, the territory of Marina di Ginosa resulted "dry semi-arid" for all three hydrological years considered and for the whole period of analysis. Therefore, this area suffered from water scarcity in the period 2015–2018. This conclusion is consistent with the World Atlas of Desertification (WAD) [42], which states that "aridity" and "water scarcity" are biophysical issues challenges affecting this region. Furthermore, because this assessment only took three years of observations into account, and because a much longer period (at least 30 years) would be required for a more accurate evaluation of the climatic type of the area, the term "drought" could be reasonably used to define the condition of water scarcity affecting this territory from 2015 to 2018 [43–45].

Table 5. FAO-UNEP aridity index calculated for the period of analysis, and climate classification.

Year	AI	Climate type
2015–2016	0.44	Dry semi-arid
2016–2017	0.36	Dry semi-arid
2017–2018	0.32	Dry semi-arid
2015–2018	0.37	Dry semi-arid

4 Conclusion

The objective of this paper is to integrate different Copernicus and other open data for the monthly evaluation of the hydrological balance throughout the region of Marina di Ginosa, in southern Italy. To that end, a JavaScript code was written in the GEE cloud platform to calculate the primary component of the hydrological balance at a resolution of 10 m for the period 2015–2018, using the ISPRA's BIGBANG approach. Monitoring and quantitative evaluation of water resources is undoubtedly fundamental to supporting sustainable water resource management and hence decision-making in this sector, especially in light of the potential consequences of climate change and urbanization [11, 13, 14, 46–48].

Because the FAO-UNEP aridity index [13, 38–40] identifies the climate as "dry semi-arid", this research determines that this area was affected by water scarcity from 2015–2018. However, in order to correctly interpret the results, the model's simplifications and schematizations must be taken into consideration. Furthermore, to improve estimations accuracy, a greater number of precipitation and temperature measurements from nearby hydro-meteorological stations should be evaluated and interpolated using geostatistical methods.

References

1. Caretta, M.A., et al.: Water. In: Pörtner, H.-O., et al. (eds.) Climate Change 2022: Impacts, Adaptation and Vulnerability. Contribution of Working Group II to the Sixth Assessment Report of the Intergovernmental Panel on Climate Change, pp. 551–712. Cambridge University Press, Cambridge, UK and New York, NY, USA (2022)
2. Konapala, G., Mishra, A.K., Wada, Y., Mann, M.E.: Climate change will affect global water availability through compounding changes in seasonal precipitation and evaporation. Nat. Commun. **11**, 3044 (2020)
3. Haddeland, I., et al.: Global water resources affected by human interventions and climate change. PNAS **111**, 3251–3256 (2013)
4. Grillakis, M.G.: Increase in severe and extreme soil moisture droughts for Europe under climate change. Sci. Total Environ. **660**, 1245–1255 (2019)
5. Manfreda, S., Iacobellis, V., Fiorentino, M.: Appunti di idrologia superficiale, 1st edn. Aracne editrice, Roma (2010)
6. ASCE: Hydrology handbook. ASCE Manuals and Reports on Engineering Practice No. 28, 2nd edn. American Society of Civil Engineering, New York (1996)

7. Balha, A., Vishwakarma, B.D., Pandey, S., Singh, C.K.: Predicting impact of urbanization on water resources in megacity Delhi. Remote Sens. Appl.: Soc. Environ. **20**, 100361 (2020)
8. Ge Sun, C.L., et al.: Impacts of urbanization on watershed water balances across the conterminous United States. Water Resour. Res. **56** (2020)
9. Daba, M.H., Bazi, Z., Belay, A.: Effects of climate change on soil and water resources: a review. J. Environ. Earth Sci. **8**, 71–80 (2018)
10. Grusson, Y., Wesström, I., Svedberg, E., Joel, A.: Influence of climate change on water partitioning in agricultural watersheds: examples from Sweden. Agric. Water Manag. **249**, 106766 (2021)
11. Braca, G., Bussettini, M., Ducci, D., Lastoria, B., Mariani, S.: Evaluation of national and regional groundwater resources under climate change scenarios using a GIS-based water budget procedure. Rendiconti Lincei. Scienze Fisiche e Naturali **30**(1), 109–123 (2019). https://doi.org/10.1007/s12210-018-00757-6
12. Copernicus Climate Change Service: Water management. https://climate.copernicus.eu/water-management. Last accessed 31 Mar 2023
13. Braca, G., Bussettini, M., Lastoria, B., Mariani, S., Piva, F.: Il Bilancio Idrologico Gis Based a scala Nazionale su Griglia regolare – BIGBANG: metodologia e stime. Rapporto sulla disponibilità naturale della risorsa idrica. Istituto Superiore per la Protezione e la Ricerca Ambientale, Rapporti 339/21, Roma (2021)
14. Braca, G., Ducci, D.: Development of a GIS Based Procedure (BIGBANG 1.0) for Evaluating Groundwater Balances at National Scale and Comparison with Groundwater Resources Evaluation at Local Scale. In: Calvache, M.L., Duque, C., Pulido-Velazquez, D. (eds.) Groundwater and Global Change in the Western Mediterranean Area. EES, pp. 53–61. Springer, Cham (2018). https://doi.org/10.1007/978-3-319-69356-9_7
15. Moghim, S.: Assessment of water storage changes using GRACE and GLDAS. Water Resour. Manage. **34**(2), 685–697 (2020). https://doi.org/10.1007/s11269-019-02468-5
16. Jutz, S., Milagro-Pérez, M.P.: Copernicus: the European Earth Observation programme. Revista de Teledetección **56**, V–XI (2020)
17. Copernicus: Infrastructure overview. https://www.copernicus.eu/en/about-copernicus/infrastructure-overview. Last accessed 1 Apr 2023
18. Copernicus Climate Change Service. https://climate.copernicus.eu/about-us. Last accessed 31 Apr 2023
19. Thépaut, J-N., Dee, D., Engelen, R., Pinty, B.: The Copernicus programme and its climate change service. In: IGARSS 2018 – 2018 IEEE International Geoscience and Remote Sensing Symposium, pp. 1591–1593. IEEE, Valencia, Spain (2018)
20. Gorelick, N., Hancher, M., Dixon, M., Ilyushchenko, S., Thau, D., Moore, R.: Google Earth Engine: planetary-scale geospatial analysis for everyone. Remote Sens. Environ. **202**, 18–27 (2017)
21. Kumar, L., Mutanga, O.: Google Earth Engine applications since inception: usage, trends and potential. Remote Sens. **10**, 1509 (2018)
22. Barletta, C., Capolupo, A., Tarantino, E.: Exploring the potentialities of Landsat 8 and Sentinel-2 satellite data for estimating the land surface albedo in urban areas using GEE platform. In: Gervasi, O., et al. (eds.) International Conference on Computational Science and Its Applications, LNCS, vol. 13379, pp. 435–449. Springer, Cham. (2022)
23. Capolupo, A., Monterisi, C., Barletta, C., Tarantino, E.: Google Earth Engine for land surface albedo estimation: comparison among different algorithms. In: Proceedings of SPIE, vol. 11856, Remote Sensing for Agriculture, Ecosystems, and Hydrology XXIII, p. 118560F. International Society for Optics and Photonics (2021)
24. Capolupo, A., Monterisi, C., Saponaro, M., Tarantino, E.: Multi-temporal analysis of land-cover changes using Landsat data through Google Earth Engine platform. In: Proceedings of

SPIE, vol. 11524, Eighth International Conference on Remote Sensing and Geoinformation of the Environment (RSCy2020), p. 1152419. International Society for Optics and Photonics (2020)
25. Cotecchia, V.: Area idrogeologica dell'arco ionico tarantino. In: Acque sotterranee e l'intrusione marina in Puglia: dalla ricerca all'emergenza nella salvaguardia della risorsa. Memorie descrittive della carta geologica d'Italia 92, pp. 248–312. ISPRA Serv. Geologico d'Italia (2014)
26. Tropeano, M., Sabato, L., Pieri, P.: Filling and cannibalization of a foredeep: the Bradanic Trough, Southern Italy. Geol. Soc. London, Special Pub. **191**, 55–79 (2002)
27. Cotecchia, V., Simeone, V., Gabriele, S.: Caratteri climatici. In: Acque sotterranee e l'intrusione marina in Puglia: dalla ricerca all'emergenza nella salvaguardia della risorsa. Memorie descrittive della carta geologica d'Italia 92, pp. 338–369. ISPRA Serv. Geologico d'Italia (2014)
28. Copernicus Land Monitoring Service: https://land.copernicus.eu/. Last accessed 4 Apr 2023
29. Harris, I., Osborn, T.J., Jones, P., Lister, D.: Version 4 of the CRU TS monthly high-resolution gridded multivariate climate dataset. Sci. Data **7**, 109 (2020)
30. Munafò, M., Salvati, L., Zitti, M.: Estimating soil sealing rate at national level – Italy as a case study. Ecol. Ind. **26**, 137–140 (2013)
31. Ballabio, C., Panagos, P., Montanarella, L.: Mapping topsoil physical properties at European scale using the LUCAS database. Geoderma **261**, 110–123 (2016)
32. Panagos, P., et al.: European Soil Data Centre 2.0: soil data and knowledge in support of the EU policies. Eur. J. Soil Sci. **73**, e13315 (2022)
33. Panagos, P., Van Liedekerke, M., Jones, A., Montanarella, L.: European Soil Data Centre: response to European policy support and public data requirements. Land Use Policy **29**, 329–338 (2012)
34. European Commission, Joint Research Centre: European Soil Data Centre (ESDAC). http://esdac.jrc.ec.europa.eu. Last accessed 4 Apr 2023
35. Celico, P.: Prospezioni idrogeologiche. Liguori Editore, Napoli (1988)
36. Tamiminia, H., Salehi, B., Mahdianpari, M., Quackenbush, L., Adeli, S., Brisco, B.: Google Earth Engine for geo-big data applications: a meta-analysis and systematic review. ISPRS J. Photogramm. Remote. Sens. **164**, 152–170 (2020)
37. Mutanga, O., Kumar, L.: Google Earth Engine Applications. Remote Sens. **11**, 591 (2019)
38. European Commission – Joint Research Centre: World Atlas of Desertification: patterns of aridity. https://wad.jrc.ec.europa.eu/patternsaridity. Last accessed 8 Apr 2023
39. Stefanidis, K., Kostara, A., Papastergiadou, E.: Implications of human activities, land use changes and climate variability in Mediterranean lakes of Greece. Water **8**, 483 (2016)
40. United Nations Environmental Programme. World atlas of desertification. Edward Arnold, London, UK (1992)
41. Eurostat and OCSE: Data collection manual for the OECD/Eurostat joint questionnaire on inland waters and Eurostat regional water questionnaire. Concepts, definitions, current practices, evaluations and recommendations, Version 4 (2018)
42. European Commission – Joint Research Centre: World Atlas of Desertification: convergence of global change issues. https://wad.jrc.ec.europa.eu/countryreport. Last accessed 8 Apr 2023
43. NOAA: Drought vs. aridity. https://www.ncei.noaa.gov/access/monitoring/dyk/drought-aridity. Last accessed 8 Apr 2023
44. European Environment Agency: Wet and dry – aridity. https://www.eea.europa.eu/publications/europes-changing-climate-hazards-1/wet-and-dry-1/wet-and-dry-aridity. Last accessed 8 Apr 2023
45. European Environment Agency: Wet and dry – drought. https://www.eea.europa.eu/publications/europes-changing-climate-hazards-1/wet-and-dry-1/wet-and-dry-drought. Last accessed 8 Apr 2023

46. Figorito, B., Tarantino, E., Balacco, G., Fratino, U.: An object-based method for mapping ephemeral river areas from WorldView-2 satellite data. In: Proceedings of SPIE, Remote Sensing for Agriculture, Ecosystems, and Hydrology XIV, vol. 8531, p. 85310B (2012)
47. Apollonio, C., Balacco, G., Novelli, A., Tarantino, E., Piccinni, A.F.: Land use change impact on flooding areas: the case study of Cervaro Basin (Italy). Sustainability **8**, 996 (2016)
48. IDMP: Drought and water scarcity. WMO No.1284. Global Water Partnership, Stockholm, Sweden and World Meteorological Organization, Geneva, Switzerland (2022)